BULGING EFFECTS ON LONGITUDINAL CRACKS IN LAP JOINTS OF PRESSURIZED AIRCRAFT FUSELAGE

Anisur Rahman
NAVAIR, North Island
Tactical Aircraft Strength Branch
Code 4.3.3.1.0
San Diego, CA

John G. Bakuckas, Jr., Paul W. Tan, and Catherine A. Bigelow, AAR-400
FAA William J. Hughes Technical Center
Atlantic City International Airport, NJ

Abstract

Longitudinal cracks in a pressurized aircraft fuselage structure are subjected to complex stress and displacement fields resulting in nonlinear out-of-plane deformations. This so-called bulging effect can significantly elevate the stress-intensity factor (SIF) at the crack tip and reduce the residual strength. One way to measure the bulging effect is by the bulging factor, which is the ratio of the SIF of a longitudinal crack in the curved fuselage to the SIF for the same crack in a flat panel. The damage tolerance design philosophy requires determination of realistic stress state in the vicinity of cracks in airframe fuselage structure. However, most studies of bulging effects are for idealized unstiffened shells. Few studies have been conducted to study the significance of bulging effects on cracks in lap joints of aircraft fuselage structure and the consequence of not including these effects in the stress predictions and subsequent damage tolerance analysis. An area of particular concern is the critical rivet row in a longitudinal lap splice joint, 1 of the 16 critical areas identified by the Airworthiness Assurance Working Group as having the potential for fatigue crack initiation. This study was undertaken to examine the effects of bulging of a midbay crack in the critical row of a longitudinal lap splice joint. A typical transport class aircraft fuselage was modeled. The bulging factors were calculated using a nonlinear finite element analysis. The SIF at the crack tip were calculated using the Modified Closure Integral method. The loading, crack length, and stiffening elements (frames and stringers) were varied. In general, results reveal that the bulging phenomenon occurred in the typical longitudinal lap joint considered, even with stiffening elements.

Introduction

The evolution of cracks in a pressurized fuselage structure is a complex process due to biaxial and internal pressure loads and the structural configuration. The response of such cracks is characterized by large out-of-plane deformations or bulging of the surfaces of the crack, as illustrated in Figure 1, which develop local membrane and bending stresses. The bulging phenomena is often quantified in terms of a bulging factor defined as the ratio of the stress-intensity factor (SIF) of a crack in a curved panel to the stress-intensity factor of the same crack in a flat panel:

$$\beta = \frac{K_{curved}}{K_{flat}} \tag{1}$$

Thus, the bulging factor, β, is a geometry factor, which can be applied to the SIF of a crack in a flat plate to obtain the SIF for the same crack in a curved shell. To accurately determine the effect of crack bulging on crack growth in curved structures, calculations of the bulging factors for the fuselage configurations

used in industry are needed. The bulging factor is a nonlinear function of the applied pressure, material properties, and geometric parameters, including the fuselage radius, fuselage thickness, and crack length. To accurately model bulging cracks, including the out-of-plane deformation, a large displacement theory and geometric nonlinearties must be considered.

Several studies have been conducted to characterize bulging cracks [1-6]. However, most work done to date has been for unstiffened shells. Early works of Folias [1] provided the first analytical expressions for bulging factors based on linear elastic theory. Numerical analysis by Erdogen and Kibler [2], using linear elastic fracture mechanics, support the expressions developed by Folias.

However, later work conducted by Riks [3] and Ansell [4], using geometric nonlinear finite element analysis, demonstrated that the bulging phenomena was a nonlinear problem and that large deformations need to be considered in order to appropriately characterize bulging cracks. It was shown that the SIF for a given crack configuration increased with applied pressure and the value was smaller than the value using linear elastic theory. The work of Chen and Schijve [5] considered the problem from a fracture mechanics, energy balance approach accounting for the nonlinear deformation in the vicinity of the crack using a semiempirical formulation. By correlating with experiments, Chen and Schijve [5] developed an expression for the bulging factor that was in good agreement with the results published by Riks [3] and Ansell [4].

Due to the complexities of analyzing bulging cracks, a wide range of SIFs for bulging cracks are not available. Without SIFs, accurate damage tolerance assessments for a broad spectrum of crack configurations in aircraft fuselage structures are difficult. Only a handful of studies have been done for stiffened shells [3-6]. One of these was carried out by the Federal Aviation Administration (FAA), in which Bakuckas, et al. [6] investigated the effect of bulging on curved panels that were both unstiffened and stiffened with straps. The present study builds upon this work and looks into the effect of bulging on a cracked longitudinal lap splice joint. An area of particular concern is the critical rivet row in the longitudinal lap splice joint, which is 1 of the 16 critical areas identified by the Airworthiness Assurance Working Group (AAWG) as susceptible to widespread fatigue damage (WFD) [7]. No published solutions for bulging factors for cracks in a longitudinal lap splice joint exist. In the current study, a typical fuselage with a longitudinal lap splice joint with a crack in its critical rivet row was selected, shown in Figure 1. The effects of the presence of the lap splice, the stringers, and the frames on the bulging factor were examined. The current results will help in evaluating the need to incorporate bulging factors in the damage tolerance studies and residual strength analysis of fuselages.

Computational Methodology

Computing the Bulging Factor

In this study, the mixed-mode SIFs were calculated using the Modified Crack Closure Integral (MCCI) method. In the MCCI method, it is assumed that the energy released during crack extension is the same as the work that would be needed to close the crack. This work is set equal to the energy release rate, from which the SIFs are calculated. Corresponding to each mode of deformation, the energy released can be partitioned into four components and the SIF for each mode is calculated [8-10]. The four SIF components consist of two in-plane stress-intensity factors, K_1 and K_2, due to the opening or tension mode and the shearing mode, respectively. The other two stress-intensity factors, k_1 and k_2, called the Kirchoff stress-intensity factors, are due to the symmetric bending and unsymmetric bending loads, respectively. The loading modes are shown in Figure 2. A detailed description of the MCCI method can be found in Reference 9. In all the cases studied, the Mode I SIF, K_1, was the most dominant of the four SIFs, and this was the component that was used to determine the bulging factor. Thus, in this study, the bulging factor was expressed by:

$$\beta = \frac{\boldsymbol{K}_{1\ curved}}{\boldsymbol{K}_{1\ flat}} \tag{2}$$

where, $K_{1\,curved}$ is the Mode I SIF for a crack in the curved fuselage panel, and $K_{1\,flat}$ is the Mode I SIF for the same crack configuration in an infinite flat panel under a remote tensile stress equal to the hoop stress in the curved panel:

$$K_{1\,flat} = \frac{pR}{t}\sqrt{\pi a} \tag{3}$$

Here a is the half crack length, p is the internal pressure, R is the fuselage radius, and t is the skin thickness.

Verification Studies

To verify the computational approach and to insure sufficient fidelity in the finite element mesh, a problem with a known solution was modeled first: a pressurized unstiffened cylinder with a radius R of 64.96 in. (1650 mm). The cylinder was made of 2024 aluminum alloy with a thickness (t) of 0.0394 in. (1 mm). A longitudinal crack of length $2a$ = 7.874 in. (200 mm) was modeled. The solution of this problem can be obtained from the work of Bakuckas [6] and Chen [5, 11]. Bakuckas solved the problem using a geometrically nonlinear finite element method with a global local hierarchical finite element approach and used the J-integral to calculate the SIF. Chen combined the analytical results of Ansell [4] and Riks [3] with test results and presented the bulging factors in the form of a semiempirical equation given by:

$$\beta = \sqrt{1 + \frac{5}{3\pi}\frac{\boldsymbol{Eta}}{\boldsymbol{R^2 p}} \cdot 0.316 \tanh\left(0.06 \cdot \frac{\boldsymbol{R}}{\boldsymbol{t}} \cdot \sqrt{\frac{\boldsymbol{pa}}{\boldsymbol{Et}}}\right)} \tag{4}$$

Here, E is the tensile modulus of the cylindrical shell, t is the thickness, R is the radius of curvature, p is the internal pressure, and a is the half crack length.

In the verification studies, the finite element analysis was done using ABAQUS [12]. The MCCI method was used to obtain the Mode I SIF (K_1), and equation (2) was used to calculate the bulging factor. Figure 3 shows the plot of the bulging factor as a function of pressure. These solutions are within 1% of the values reported by Bakuckas and that obtained from Chen's semiempirical equation given by equation (4), thus verifying the approach used.

Geometry and Configuration

Once the procedure was verified, the methodology was used to analyze bulging effects in a fuselage structure typical of a transport category aircraft. In this study, for all analyses, a representative fuselage radius of 80 in. was used with a skin thickness of 0.048 in. Four fuselage configurations, as shown in Figure 4, were studied. The first configuration was an unstiffened fuselage with a longitudinal crack, without a lap splice joint or stiffeners. The second configuration was an unstiffened fuselage with a longitudinal lap splice joint; three rows of rivets were used in the lap joint. The rivet pitch was 1 in. with a half-inch edge distance. The rivets were modeled with a circular cross section and a diameter of 0.1875 in. A crack was placed in the critical outer rivet row of the lap splice joint. In the third configuration, the fuselage with the longitudinal lap splice joint was stiffenened with stringers (longitudinal stiffening element). A stringer was placed in the middle rivet row of the lap joint. For the fourth configuration with a lap joint, the fuselage was stiffened with both stringers and frames (hoop-stiffening element). For this fully stiffened configuration, the crack was placed at a midbay location.

The stiffener configurations were selected to represent a typical transport category aircraft. The stringers were spaced at 10-in. intervals, and the frames were spaced 20 in. apart. The stringers have a hat configuration, and the frames have a Z-configuration. The schematic of the cross-sections are shown in Figure 4. The stiffeners were characterized using a stiffening ratio that relates the cross-section area of the stiffener to the skin thickness and stiffener spacing. This quantity has been identified as having the most influence on the SIF and, hence, the bulging factor in the global sense [4]. The stiffening ratio is given by:

$$\gamma = \frac{A_s}{A_s + Lt} \tag{5}$$

where A_s is the stiffener cross-sectional area, L is the stiffener spacing, and t is the skin thickness. The cross-sectional area for the frames was 0.24 in^2 and for the stringers 0.17 in^2. A stiffening ratio of 0.2 was used for frames and 0.26 for stringers.

Six different crack lengths were studied in this work, a = 1, 2, 4, 6, 8, 10, and 12 in. A total of 22 different cases were analyzed. The rivets located on the crack were assumed to be completely broken and unable to carry any load. In the fully stiffened configuration, the crack was located midbay. The crack was grown by generating additional nodes in front of the crack tip and splitting the elements.

Finite Element Models

A geometrically nonlinear finite element analysis was conducted using the commercial finite element package ABAQUS [12]. Finite element models were developed for each of the four configurations shown in Figure 4. A typical finite element mesh for the fully stiffened fuselage is shown in Figure 5. For this case, approximately 23,000 elements were used. The fuselage skin was modeled using 4-noded shell elements with reduced integration. The stiffeners (stringers and frames) were modeled using beam elements having the cross-sectional properties discussed above and shown in Figure 4. Beam elements were used to model the rivets that connected the substructures with the skin and the substructures to one another. To simplify the modeling, the rivet holes were not modeled. The semi-empirical equation developed by Swift [13] was used to calculate the shear stiffness of the beams where the rivet shear stiffness is given by:

$$k_{shear} = \frac{E'd}{5 + 0.8\left(\frac{d}{t} + \frac{d}{t_s}\right)} \tag{6}$$

Here, $E' = 10.5\times10^6$ psi is the skin modulus, d = 0.1875 in. is the rivet diameter, t = 0.048 in. is the thickness of the first skin, and t_s = 0.048 in. is the thickness of the second skin. Table 1 lists the mechanical properties [14] used for skin, doublers, frames, and stringers.

The crack configurations were simulated using pairs of coincident nodes along the shared edges of two rows of elements, as shown in the detailed view in Figure 5. An orthogonal mesh was used in the immediate vicinity of the crack tips where the size of the elements were at least 0.25 in.

The boundary conditions applied are shown in Figure 5. Taking advantage of symmetry, only half of the panels were modeled. Symmetry conditions were applied on the two longitudinal edges and one hoop edge perpendicular to the crack face, and at the center of the crack. For the remaining side, only the rotations about the z- and θ axes were constrained. Internal pressure was applied to the inner surface of the skin elements. The pressure was applied incrementally, loading the model to 10 psi, and the bulging factor was calculated at each increment.

Results and Discussion

The results are presented in terms of the bulging factor, β, as a function of applied internal pressure. The first set of analyses is for the baseline configuration, an unstiffened fuselage with a central crack. The bulging factor for this configuration is plotted as a function of internal pressure, as shown in Figure 6. Results show, that for all crack lengths, the bulging factor decreases as pressure increases. This nonlinearity has been attributed to the straightening or tightening of the crack in the hoop direction as the pressure increases, which also has been reported by other authors [3, 4, 6, 11]. The variation of the bulging factor increases as the crack length increases. For the smallest crack length analyzed (a = 1 in., where a is the half-crack length), the bulging factor is practically constant at 1.2; whereas, for the longest

crack length analyzed (a = 8 in.), the bulging factor varies between 2.5 and 4.0 for the pressure considered. Thus, the bulging phenomenon in unstiffened cylindrical shells becomes more geometrically nonlinear as the crack grows.

Figure 7 depicts the results for the analyses of the unstiffened fuselage configuration with a longitudinal lap splice joint. The crack was placed in the outermost critical rivet row. Five different cracks with half lengths of a = 1, 2, 4, 6, and 8 in. were considered. The trends in the bulging factor plots are similar to the baseline case shown in Figure 6, but the values are slightly lower. The presence of the riveted lap splice shields the crack and provides some stiffening effect. Compared to the baseline case, at an applied pressure of 10 psi, the bulging factor decreased 16% and 5% for a crack length of a = 1 and 8 in., respectively. The stiffening effect of the lap splice is less significant at longer crack lengths and also as the applied pressure increases.

The next set of results are for the longitudinally stiffened lap joint shown in Figure 8. For this case, the stringer spacing is 20 in. The presence of stringers provides additional stiffness to the configuration. In the configuration analyzed, the lap splice stringer runs parallel to the crack at a distance of one rivet pitch. This stringer locally resists the out-of-plane deformation of the crack faces, resulting in a decrease in bulging factor compared to unstiffened baseline and lap splice cases. This local effect increases as the crack length increases. A nearly constant decrease in the bulging factor was obtained for all crack lengths analyzed. Compared to the baseline case, the bulging factor was reduced by 26% and 29% for a crack length of a = 1 and 8 in., respectively.

In the final set of analyses, the fuselage was stiffened in both the longitudinal and hoop directions. The bulging factors for this configuration are presented as a function of pressure in Figure 9. Here, seven different crack lengths were considered, a = 1, 2, 4, 6, 8, 10, and 12 in., and the frame spacing was 20 in. Thus, the smallest crack analyzed, a = 1 in., is quite remote from the frames. A crack of a = 10 in. is equal to the width of the bay, and a = 12 in. represents a crack that is wider than the bay. For crack lengths longer than the frame spacing, the frame remained intact. The addition of the frames added stiffeness to the fuselage and reduced the bulging factor compared to the results obtained for the previous longitudinally stiffened case. The effect of the frames increased for longer crack lengths. For the smallest crack analyzed, a = 1 in., where the crack was quite remote from the frame, the bulging factor was reduced by 7% at p = 10 psi compared to the longitudinally stiffened case. The longer the crack, i.e., the crack tip is closer to the frame, the greater the reduction in the bulging factor. For a = 8 in., the reduction is almost 13% compared to the longitudinally stiffened case. At a given pressure, the magnitude of the bulging factor increased with the crack length up to a = 10 in. when the crack is of the same length as the frame spacing. For cracks longer than the frame spacing, the bulging factor actually decreased due to the stiffening effect of the intact frame. Similar phenomenon was observed by Bakuckas, et al. [6] for bulging cracks in stiffened shells with hoop tear straps.

The effect of configuration on the bulging factor is summarized in Figures 10 and 11 for crack length, a = 1 and 8 in., respectively. For the configurations analyzed, bulging factors were the highest for the baseline case and then reduced with each additional stiffening element. In all cases, the lap joint provided some stiffening effect, reducing the bulging factor compared to the baseline case. In addition, the results from longer cracks exhibit more geometric nonlinearity than results from shorter cracks. As shown in Figure 10, for shorter crack lengths, response is nearly constant with small incremental reductions in the bulging factor with the addition of stringers and frames. In this case, the crack is too small and too far from the stiffening elements to be affected by them. Figure 11 shows the effect of configuration for a longer crack, a = 8 in. In this case, the bulging factor is a nonlinear function of the applied pressure. In addition, the crack was long enough to be influenced by the stringers and frames. As shown in Figure 11, there is a substantial reduction in the bulging factor for the longitudinally stiffened cased compared to the unstiffened lap joint case.

Finally, Figure 12 shows the mixed mode SIFs as a function of the applied pressure for the longitudinally stiffened case with a crack length a = 8 in. The four components of SIF are the Mode I SIF caused by tensile load, K_1; the Mode II SIF cause by in-plane shear load, K_2; the SIF due to symmetric bending loads, k_1; and the SIF due to out-of-plane shear and twist loads, k_2. As shown, K_1 is the dominant mode compared to the other modes of SIF. The next highest SIFs, K_2 and k_2, were not significant.

Concluding Remarks

In this study, the effects of bulging in aircraft structures containing a longitudinal lap splice joint were determined. A typical three-rivet row lap joint configuration containing a midbay crack in the critical rivet row was chosen and analyzed. The Modified Crack Closure integral method was used to calculate crack tip stress-intensity factors (SIF). The Mode I SIF was dominate, compared to the other modes and was used in calculating the bulging factor. Parametric studies were done to examine the effects of crack length, applied pressure, and stiffening elements (stringers and frames) on the bulging factor. For short cracks, a near-constant response was obtained for the bulging factor as a function of the applied pressure. The presence of the stiffeners only slightly reduced the bulging factor for the shorter cracks. These cracks are too small and too far from the stiffening elements to be affected by them. For longer cracks, the bulging factor varied nonlinearly as a function of the applied pressure. The presence of the stiffeners significantly reduced the bulging factor but not to the level that bulging can be neglected.

Acknowledgement

This work was partially supported by National Computational Science Alliance and used the Silicon Graphics Origin 2000 Distributed Shared Memory System at University of Illinois at Urbana-Champain. The first author would like to express sincere appreciation to the FAA William J. Hughes Technical Center for support through Grant (00-G-030) to Drexel University.

REFERENCES

1. Folias, E. S., "An Axial Crack in a Pressurized Cylindrical Shell," *International Journal of Fracture Mechanics*, Vol. 1, pp. 104-113, 1965.

2. Erdogan, F. and Kibler, J. J., "Cylindrical and Spherical Shells with Crack," *International Journal of Fracture Mechanics*, Vol. 5, pp. 229-237, 1969.

3. Riks, E., "Bulging Cracks in Pressurized Fuselages: A Numerical Study," NLR MP-87058-U, National Aerospace Laboratory, NLR, The Netherlands, 1987.

4. Ansell, H., "Bulging of Crack Pressurized Aircraft Structure," LUI-TEK-LIC-1988:11, Institute of Technology, Department of Mechanical Engineering, S-581 83 Linköping, Sweden.

5. Chen, D. and Schijve, J., "Bulging of Fatigue Cracks in a Pressurized Aircraft Fuselage," Report LR-655, May 1991, Faculty of Aerospace Engineering, Delft University of Technology, Delft, The Netherlands.

6. J. G. Bakuckas, P. V. Nguyen, C. A. Bigelow, and D. Broek, "Bulging Factors for Predicting Residual Strength of Fuselage Panels," *Proceedings of the Symposium - International Committee on Aeronautical Fatigue*, Vol. 1, Edinburgh, UK: EMAS, 1997.

7. Airworthiness Assurance Working Group (AAWG) report *Recommendations for Regulatory Action to Prevent Widespread Fatigue Damage in the Commercial Airplane Fleet,* revision A, June 29, 1999, J. McGuire and J. Foucault, Chairpersons.

8. M. J. Viz, A. T. Zehnder, and J. D. Bamford, "Fatigue Fracture of Thin Plates Under Tensile and Transverse Shear Stresses," *Fracture Mechanics: 26th Volume, ASTM STP 1256*, W. G. Reuter, J. H. Underwood, and J. James C. Newman, eds., Philadelphia, PA: American Society for Testing and Materials, 1995.

9. M. J. Viz, D. O. Potyondi, and A. T. Zehnder, "Computation of Membrane and Bending Stress-Intensity Factors for Thin Cracked Plates," *International Journal of Fracture*, vol. 72, pp. 21-38, 1995.

10. E. F. Rybicki and M. F. Kanninen, "A Finite Element Calculation of Stress-Intensity Factors by a Modified Crack Closure Integral," *Engineering Fracture Mechanics*, vol. 9, pp. 931-938, 1977.

11. D. Chen, "Bulging of Fatigue Cracks in a Pressurized Aircraft Fuselage," Ph. D. Dissertation, *Department of Aerospace Engineering*. Delft, The Netherlands: Delft University of Technology, 1991.

12. ABAQUS, 5.8 ed., Pawtucket, RI 02860: Hibbitt, Karlsson, and Sorenson (HKS), 1998.

13. Swift, T., "Development of the Fail-Safe Design Features of the DC-10," *American Society for Testing and Materials Special Technical Publication 486*, 1970, pp. 164-214.

14. "Metallic Materials and Elements for Aerospace Vehicle Structures," MIL-HDBK-5H, Change Notice 1, October 2001.

Table 1. Mechanical Properties referenced form MIL-HDBK-5H [14]

Component	Material	Thickness (in)	Modulus of Elasticity (ksi)	Poisson's Ratio
Skin	2024-T3	0.048	10500	0.33
Stringer	7075-T6	0.048	10300	0.33
Frame	7075-T6	0.048	10300	0.33

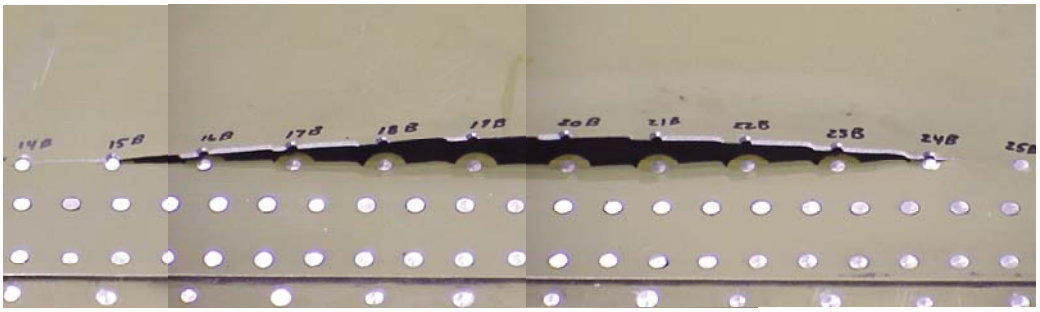

a. Crack in outer rivet row of lap splice joint

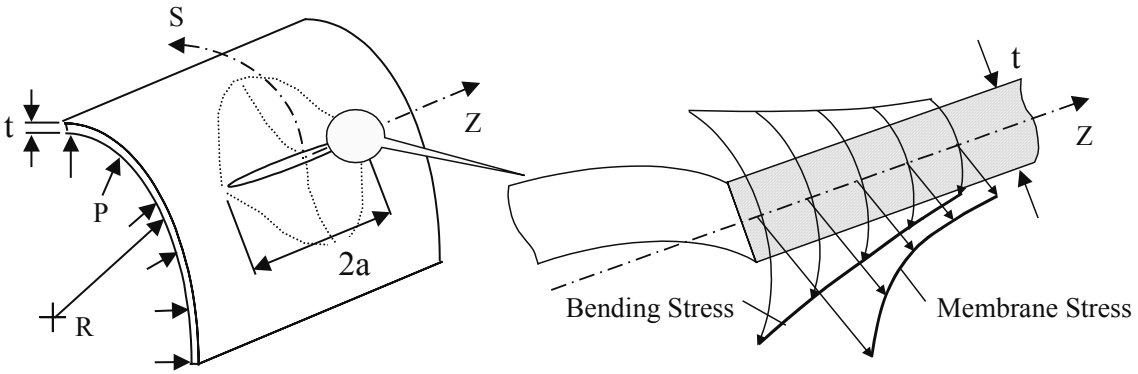

b. Bulging crack due to pressure

c. Stresses on crack plane

Figure 1. Crack bulging phenomena

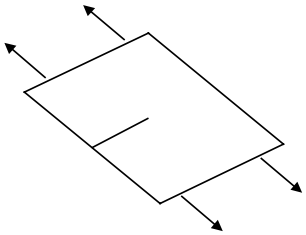

Symmetric Membrane Loading, K_1

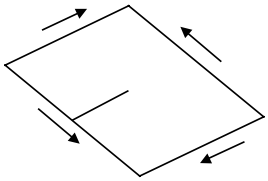

Anti -Symmetric Membrane Loading, K_2

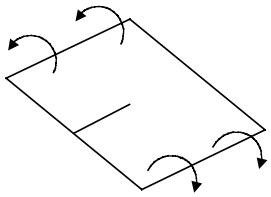

Symmetric Bend Loading, k_1

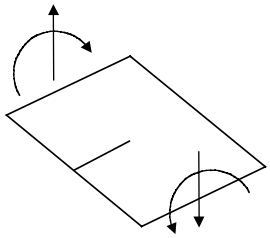

Anti -Symmetric Bending and Shear Loading, k_2

Figure 2. Kirchoff Stress-Intensity Factors

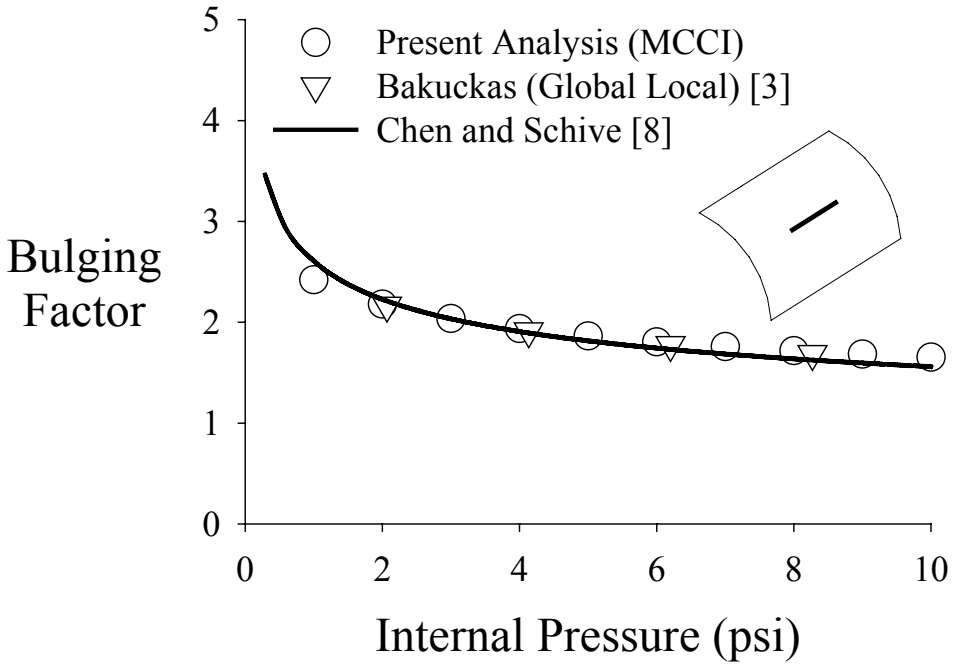

Figure 3. Comparison of bulging factor obtained by MCCI method with that obtained by other methods

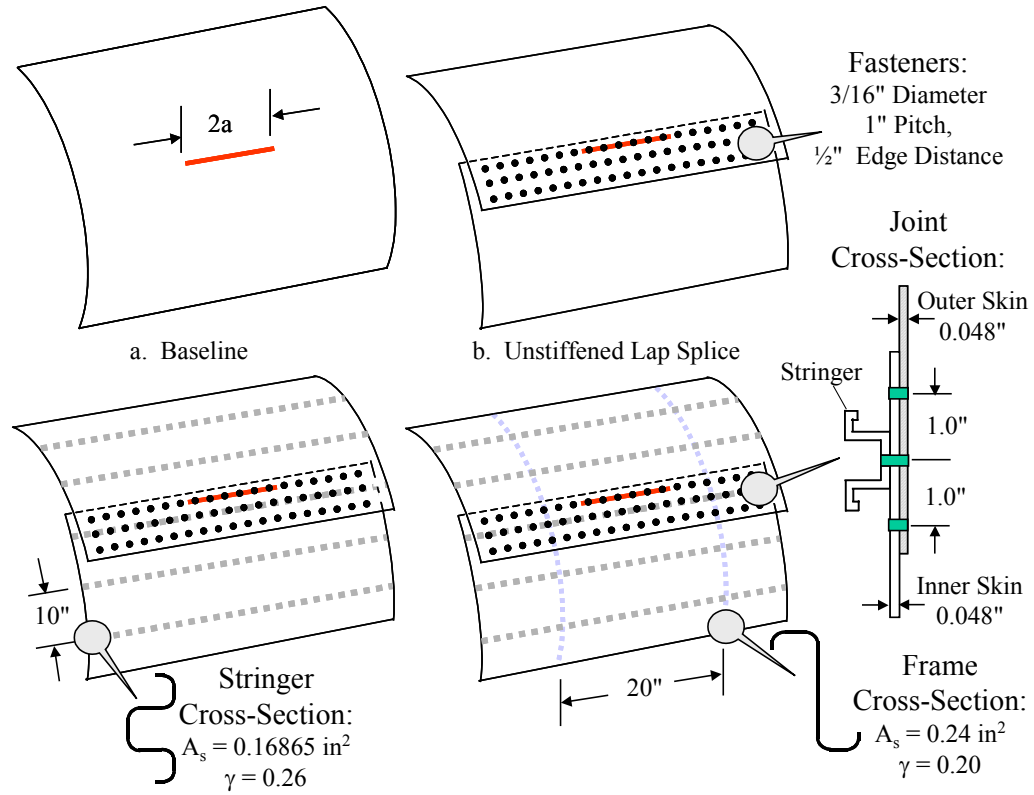

Figure 4. Fuselage configurations analyzed

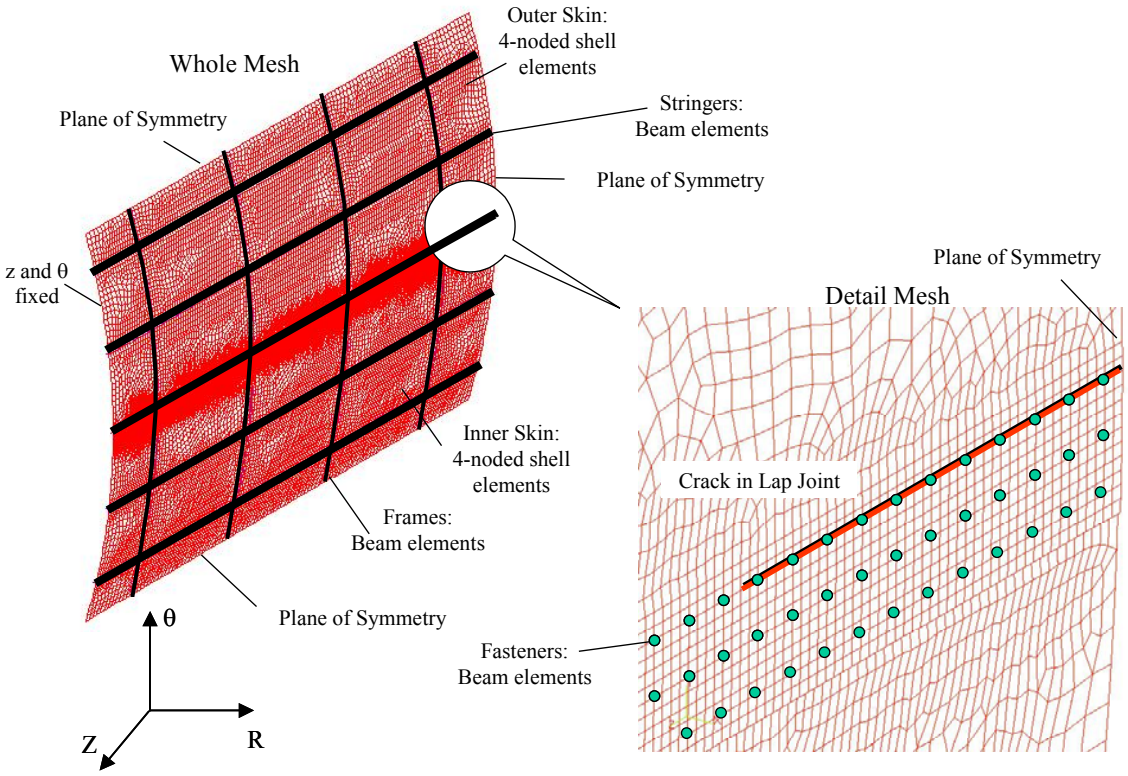

Figure 5. Finite element mesh

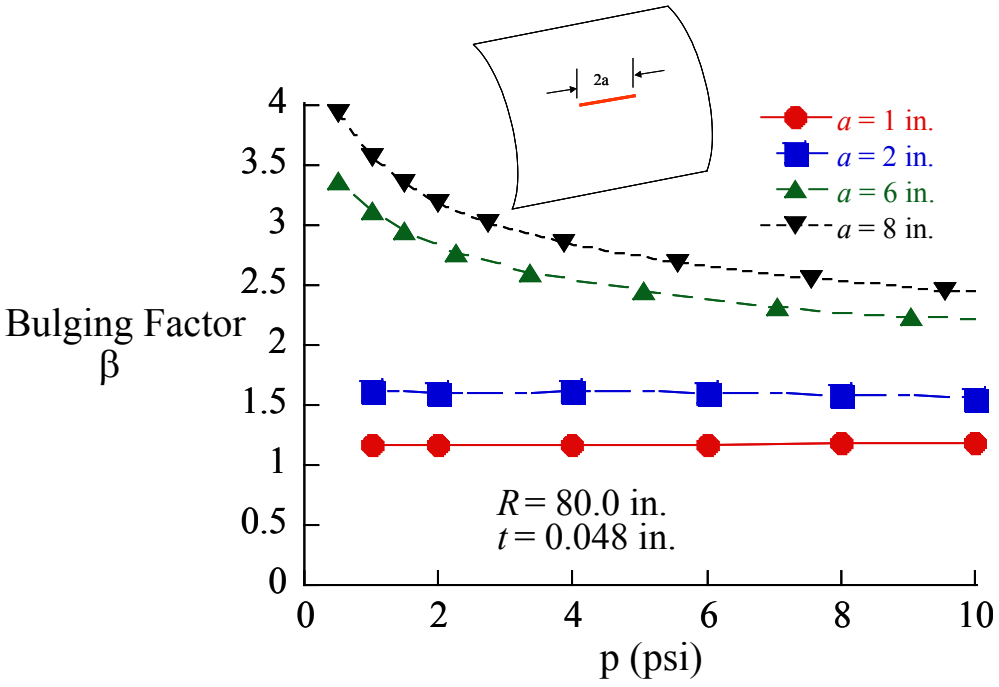

Figure 6. Bulging factors for longitudinal cracks in an unstiffened shell

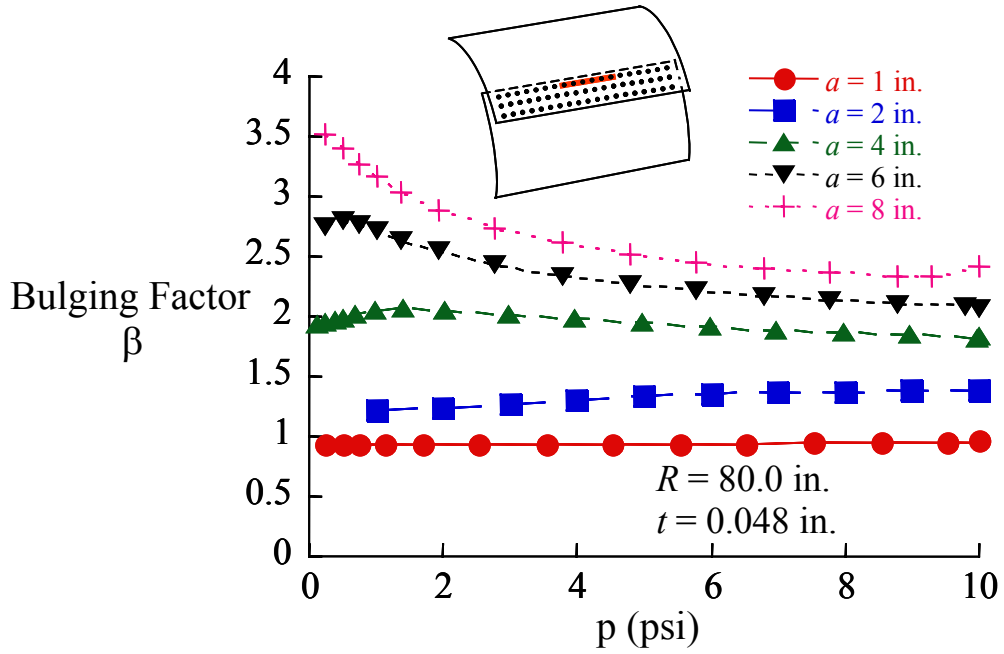

Figure 7. Bulging factor for a longitudinal crack in the critical rivet row of an unstiffened shell with a longitudinal lap splice joint

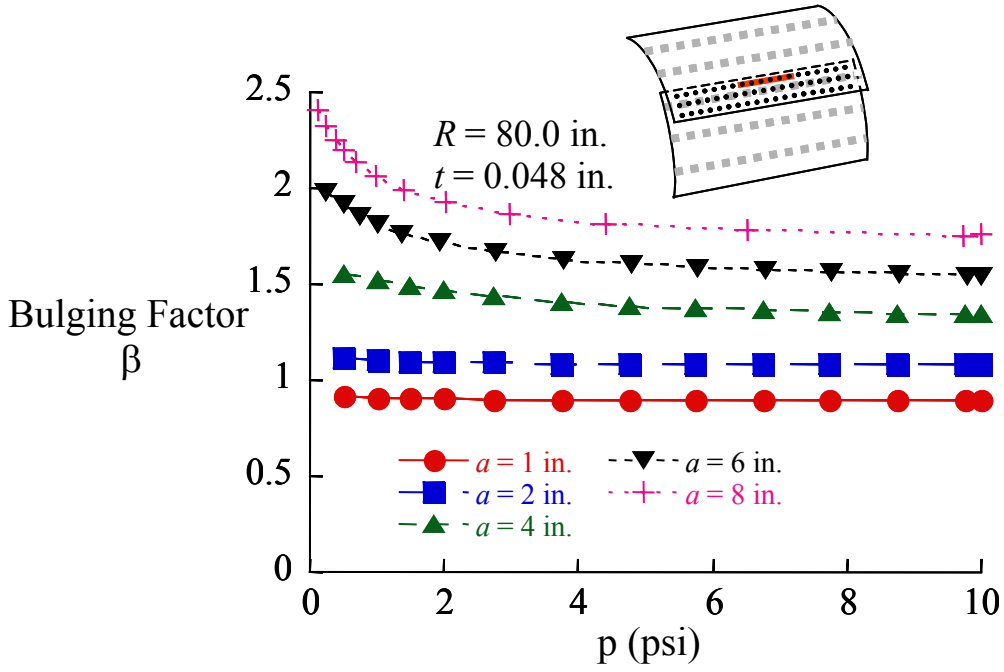

Figure 8. Bulging factor for a longitudinal crack in the critical rivet row of a longitudinally stiffened shell with a longitudinal lap splice joint

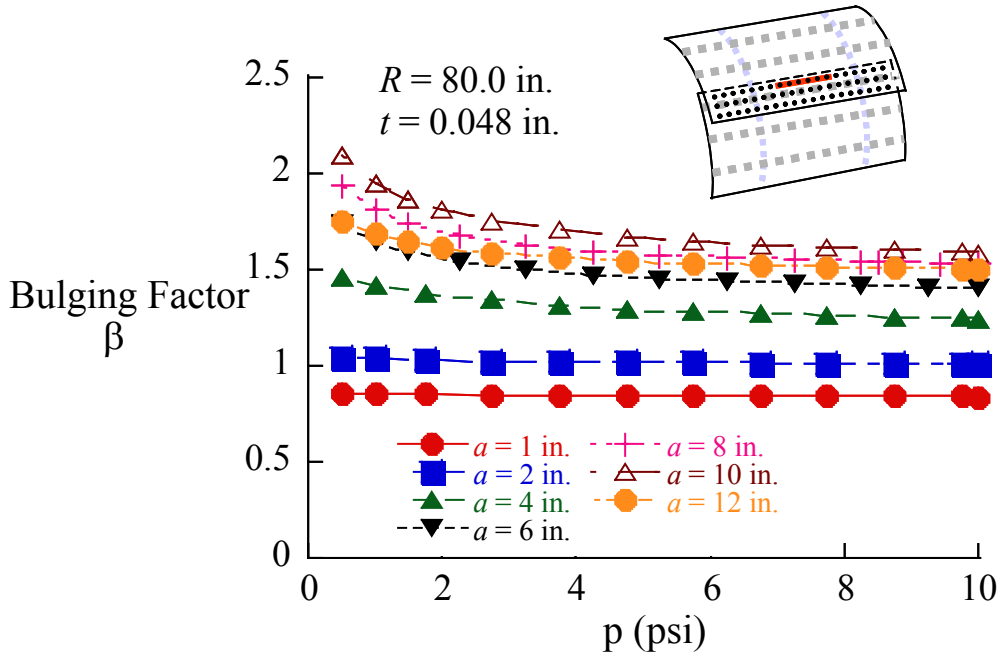

Figure 9. Bulging factor for a longitudinal crack in the critical rivet row of a fully stiffened shell with a longitudinal lap splice joint

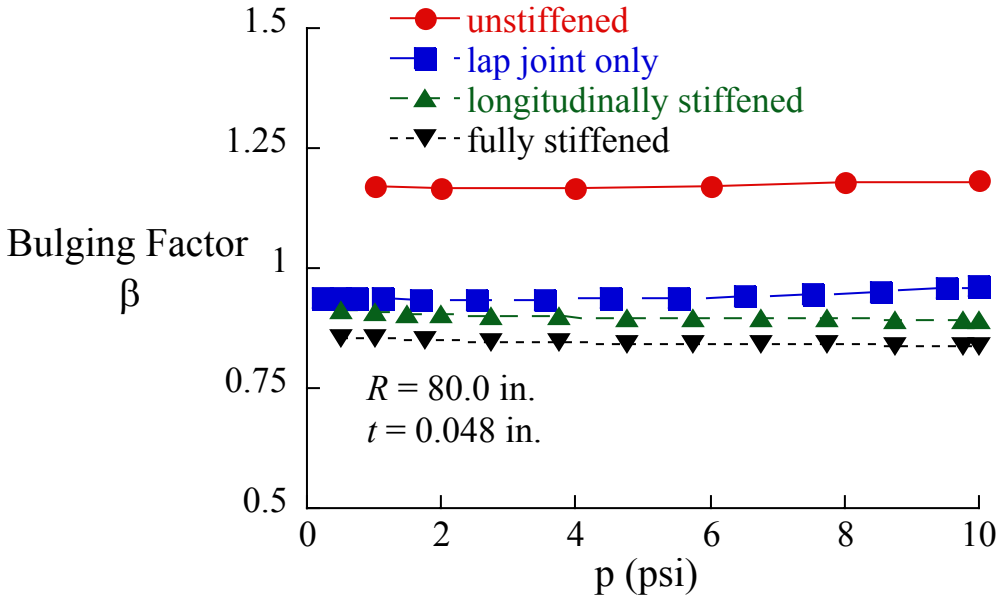

Figure 10. Bulging factor for a longitudinal crack with a = 1 in. for the configurations analyzed

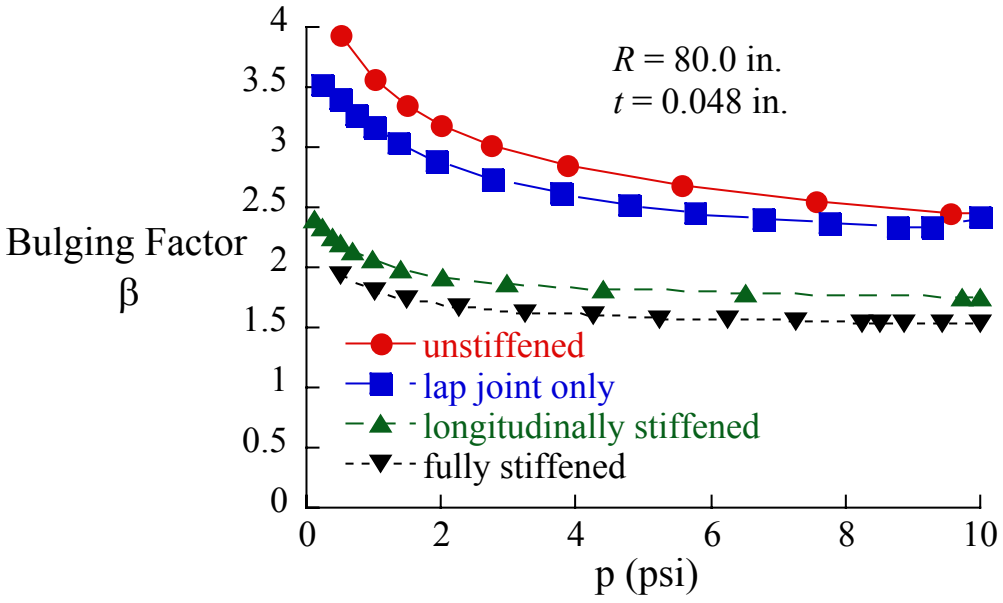

Figure 11. Bulging factor for a longitudinal crack with a = 8 in. for the configurations analyzed

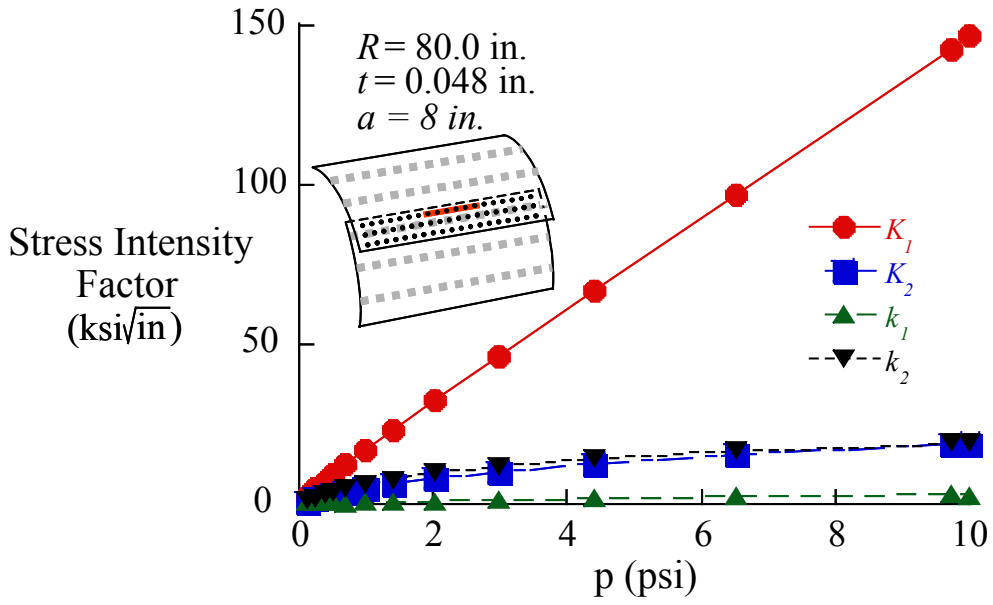

Figure 12. SIF as a function of internal pressure for a longitudinally stiffened panel with a crack length a = 8 in